



Formability Evaluation of AA 6061 Alloy Sheets on Single Point Incremental Forming using CNC Vertical Milling Machine

C. Pandivelan* and A.K. Jeevanantham

Manufacturing Division, School of Mechanical and Building Sciences, VIT University, Vellore - 632014, Tamil Nadu, India.

Received 13 Oct 2014, Revised 27 Feb 2015, Accepted 27 Feb 2015

* *Email: cpandivelan@yahoo.com, Phone: +91 9442222956*

Abstract

In this work, Single Point Incremental Forming (SPIF), a state of art technique, was carried out on Aluminum AA 6061 alloy sheets and its forming limit was determined experimentally. The straight groove and cupping tests were carried using ball ended tool in CNC vertical milling machine. In order to investigate the effects step depth and depth of groove on formability, the straight groove and cupping tests were conducted. Straight grooves were performed along the rolling and transverse directions. The sum of major strain and minor strain as a measure of formability was measured. The forming limit diagrams (FLD) for straight groove and cupping tests were plotted. Moreover the effect of anisotropy of SPIF in rolling and transverse directions was confirmed through the straight groove test. It is also found that the formability decreases as the step depth increases during the SPIF.

Keywords: Single point incremental forming; Forming limit diagram; Formability; Sheet metal forming.

1. Introduction

Sheet metals are manufactured by the rolling processes. Sheet metals have various applications starting from a simple sheet metal tray to complicated parts used in aircraft, automotive, construction. The other applications are house hold appliances, food and beverage containers, boilers, kitchen equipment, office equipment etc. A flat sheet metal is formed into complicated shapes by using the die and punch. The sheet metals are ductile in nature. They can be formed only to a certain limit. Beyond this limit failures like necking and fracture occur. The strain at the failure is called forming limit strain. It is a measure of formability of sheet metals. The conventional sheet metal forming uses the punch and die. It results in less limiting strain. It involves various problems like friction between die and sheet metal, difficulty in lubrication, high severity of forming. This is due to complicate shapes of the component produced. Moreover, the cost of the die and punch is also high. The press forming processes for sheet metal forming is limited due to the formation of necking, fracture, wrinkling or earing. The strain values are measured at the onset of these failures under tension-tension region, tension-compression region and plane strain regions. These are used to construct the Forming Limit Diagram (FLD). The FLD is an effective tool to study the formability of sheet metals. It gives the limiting strain under all strain conditions [1]. The FLD is also influenced by strain paths, blank holding pressure, and severity of forming process, friction and lubrication.

The conventional press forming processes become costlier for small batch production. This is due to the dedicated punch & die, hydraulic press and skilled tool designer. In conventional forming, the varying strain path and severe strains reduces the formability of complex shapes. These problems can be rectified in incremental sheet forming. In Single Point Incremental Forming (SPIF), a ball ended forming tool is moved in user specified paths. It incrementally develops a desired shape [2]. Since the total deformation is incrementally achieved, the limiting strain is increased.

The Incremental sheet forming (ISF) eliminates the use of die and punch. The amount of friction between forming tool and sheet metal is very less in incremental forming. Of course, the deformation is incremental, local in nature and gradual. These enhance the limiting strain during ISF. It is an growing process. Therefore, a wide analysis is required to develop the theory of incremental forming. In the present stage, only

less number of research works has been carried out in this area. Myoung shim and Jiong-jin park [3] have found the incremental formability of Al 1050. They have used PAM-STAM software package to analyse the behaviour of incremental forming. Matteo Strano [4] used a robotic cell for the ISF of AA 1050-O alloy sheets with 0.6 mm thickness. They studied the effect of process parameters. Hiroki Takano et al.[5] considered another Aluminum alloy, Al 1050 H4. They flattened and recycled the wastage from this material. They also formed it incrementally to construct FLD. They found that the recycled material shows FLD on par with that of fresh sheet. Even Aluminium foils are micro-formed successfully by incremental forming technique. A CNC machine was successfully used to microform the aluminium foils using pointed tools [6 and 7]. Kim and Park [8] studied the effect of process parameters on the ISF of Al 1050. They analysed the process using PAM-STAMP. Kopac and Kampus [2] followed various methods to form the sheet metals incrementally using CNC machine. Park and kim [9] attempted to form the complex shapes. They also analyzed its incremental formability. In continuation of this, Kim and Yang [10] attempted to improve the incremental formability. They became successful by using double pass method in CNC milling machine. Aluminum alloys were formed by electro-magnetic assisted stamping process which is an unconventional ISF process by Okoye et al. [11]. Meier et al. [12] achieved an increased accuracy in the incrementally formed aluminum alloy products by using robot cell. Their analysis was made using ABAQUS. Apart from the direct experimental works, many researchers like Minoru Yamashita et al. [13], have attempted theoretical and numerical simulation of ISF. They all proved that this incremental forming is a worthy process. The ISF with two moving tools was attempted by Meier et al. [14] on Al-Mn alloy sheets. Roberta et al. [15] simulated a comparison between incremental deformation theory and flow rule using ABAQUS/EXPLICIT. Other than the works mentioned above, there are number of works that have been carried out by researchers on the ISF of Al alloy sheets namely: AA 1050, 1060, 2024, 3003, 3103, 5754, 5182, 5251, 6016, 6111, 7075. The other alloys on which researches have been carried on ISF are AZ 31, C101, SS 304, pure titanium, Ti6Al4V, Brass H62-H28, Copper T2-H28, Steel DS, and DDS 1050.

From the literature review, it is clear that only limited Al alloys are experimented using ISF. Also limited numbers of FLD constructions are reported for Al alloys in ISF. Aluminium and its alloys are used in aerospace, automotive, appliances, and food packaging due to their high strength to weight ratio and corrosion resistance. Aluminum–magnesium–silicon (Al–Mg–Si) alloys denoted as 6XXX series are medium strength heat treatable alloys. They have excellent formability and good corrosion resistance characteristics [16]. There has been considerable industrial interest in these alloys because two-thirds of all extruded products are made of aluminum, and 90% of those are made of 6XXX series alloys. In this series, AA6061 is one of the most widely used alloys [17]. Due to these reasons, an AA 6061 alloy sheet is considered in this research for the formability study on SPIF.

2. Materials and experimental procedure:

2.1 Sheet Metal and its chemical composition

The ISF is more suitable for the sheets having low thicknesses. Therefore, commercially available AA 6061 sheet with 1 mm thickness in annealed condition was chosen for this study. The Metalscan M2500 series spectrometer was used for the analysis of chemical composition. The results are given in Table 1. The AA 6061 alloy sheets were cut into 150×150 mm square blanks by shearing operation. One side of the blanks were grid marked by chemical etching method. The grids were circles in rectangular array. They were having a diameter of 2 mm. These grid circles were used to facilitate the strain measurement after forming.

Table 1. Chemical compositions of aluminium alloy AA 6061 sheets taken for this study.

Component	Mg	Si	Fe	Cu	Mn	Cr	Zn	Ti	Al
Weight %	0.8	0.64	0.37	0.21	0.08	0.16	0.04	0.03	Balance

2.2 Incremental Sheet Forming Machine

The SPIF can be carried out using a CNC vertical milling machine or robots. A CNC vertical milling machine shown in Figure 1 was chosen for this work. Due to the availability and the close dimensional control, this machine was chosen. The following is the specification of the machine.

Table size	:	810×400 mm
Travel	:	x-axis:510 mm, y-axis:400 mm and z-axis:400 mm
Spindle speed	:	60 - 800 rpm
Feed rate	:	1 - 7000 mm/min



Figure 1. CNC vertical milling machine.

2.3 Forming Tool

The forming tool used is shown in Figure 2. It is made up of EN 8 steel. The length tapered tool rod was is 100 mm length. The diameter at the rear end is 12 mm. The diameter of the front end is 8.5 mm. The front end is with a countersunk conical hole for a depth of 2.5 mm. A hardened steel ball is freely rotating in the conical hole. The ball having 10 mm diameter was placed at the conical hole.



Figure 2. Form tool used for SPIF

2.4 Straight Groove Test

The straight groove test was conducted using the CNC vertical milling machine. To study the incremental formability of AA 6061 alloy sheets straight groove test was conducted. The sheet was clamped using a fixture on the machine table. A rotating ball ended tool as shown in Figure 2 was mounted on the spindle of CNC vertical milling machine. The CNC Programme was prepared to form a straight groove in the sheet blank. The steps in making straight groove are as follows:

- Step: i. SPIF tool was made to touch the surface of the sheet blank.
- Step: ii. SPIF tool was made to penetrate by a programmed depth into the sheet blank.
- Step: iii. SPIF tool was made to move on a straight path to make a straight groove for about 40 mm length.
- Step: iv. SPIF tool was brought to the starting of groove and depth of penetration was increased by programmed quantity.
- Step: v. Steps iii & iv were repeated until fracture occurs in the sheet blanks.

In this work, the different incremental depths of penetration used are 0.15 mm, 0.2 mm, 0.25 mm, 0.30 mm and 0.35mm. Straight groove was made in each blank by following one particular incremental depth of penetration until the fracture occurs. The grid circle will become ellipses with no change in minor diameter for plane strain condition. The grid circle will become ellipse with larger minor diameter / larger circle for biaxial tension strain condition. The change in diameter of the grid circle printed were measured using a Brinell microscope. Then, the major strain (maximum value) and minor strain (minimum value) were calculated using the equations (1) and (2) respectively. The forming limit diagram was drawn by taking major strain in y-axis and minor strain in x axis. The SPIF's FLD is peculiar in nature. It differs from the FLD of conventional sheet metals forming processes. The experimental set up during the straight groove test is given in Figure 3. In this test, there are two locations where the fracture occurs. One location is the end of the groove. Another location is at a point along the groove between the two ends. Due to the nature of the process, biaxial strain condition is generated at the end of the groove and plane strain condition is generated between the ends of the groove.

$$\text{Major strain} = \ln\left(\frac{\text{Major axis length}}{\text{original circle diameter}}\right) \quad \dots (1)$$

$$\text{Minor strain} = \ln\left(\frac{\text{Minor axis length}}{\text{Original circle diameter}}\right) \quad \dots (2)$$

Figure 4 shows the different types of strain conditions developed in a straight groove. A sample formed by straight groove test is shown in Figure 5.



Figure 3. Straight groove test set up.

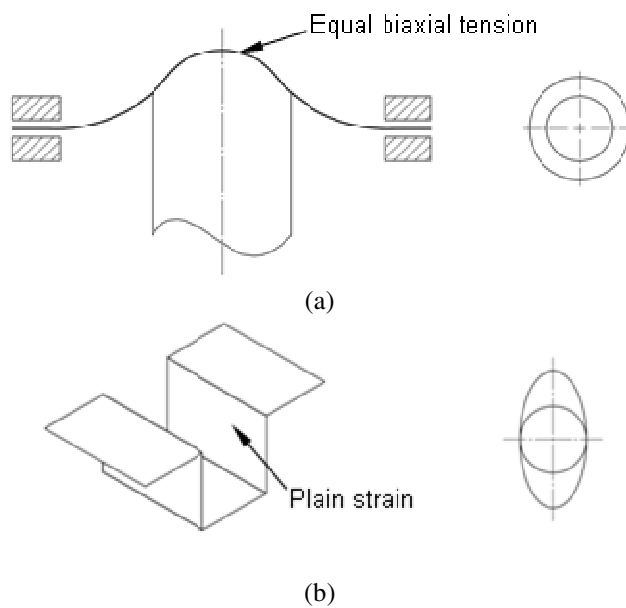


Figure 4. Strain conditions developed in straight groove test. (a) biaxial strain, (b) plain strain.



Figure 5. Sample formed in straight groove test.

2.5 Cupping Test

In cupping test, the AA 6061 sheet blank was formed into cup. The cup is a truncated cone in shape. The bottom diameter of the cup was kept at constant and the top diameter was varied. By this way, the strain condition and the wall angle of the conical cup were varied. The pattern of the tool path is shown in Figure 6. Initially, the tool was made to touch the sheet blank. Then the tool was moved in a circular path. When it reaches the starting point, the tool was given with an increment in radial and depth direction. Then, the tool was moved in circular path again. This procedure was repeated until fracture occurs. The strains were measured from the diameter of deformed circles. Using these strain values, the FLD for SPIF was plotted.

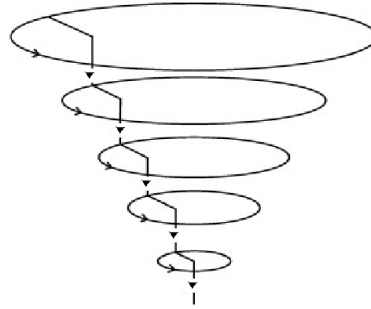


Figure 6. Pattern of tool path in cupping test.

3. Results and Discussion:

3.1 Chemical Composition

The presence of Mg and Si increases the possibility of solid solution strengthening in AA 6061. It also makes the alloy harder to small extent. The tensile and yield strengths of the Al 6061 alloy are 310 MPa and 276 MPa respectively. The flow characteristics of AA 6061 is inferior compared to pure Al due to the above reason. Still, AA 6061 is considered to have good formability in conventional die and punch forming. However, in ISF these effects will not seriously affect the formability. The Cr addition in the AA 6061 alloys increases average strain hardening exponent (n) value [18]. The average strain hardening exponent value enhances the formability in the tension-tension strain condition during forming process. Since the tension-tension strain condition dominates in the ISF process, AA 6061 alloy sheet with comparatively high Cr content will possess high incremental formability.

3.2 Straight groove test in rolling direction

Table 2 shows the major strain and minor strain in straight groove test under plane strain condition. These strain values are for different depth increments and along the rolling direction.

Table 2. Strain values for straight groove test along rolling direction under plane strain condition

Plane strain condition				
Step depth (mm)	Major diameter (mm)	Minor diameter (mm)	Major strain	Minor strain
0.15	3.831	2.04	0.65	0.02
	3.792	2.02	0.64	0.01
	3.755	2.06	0.63	0.03
0.20	3.792	2	0.64	0
	3.791	2.02	0.64	0.01
	3.717	2.04	0.62	0.02
0.25	3.607	2.02	0.59	0.01
	3.694	2.06	0.62	0.03
	3.607	2.06	0.59	0.03
0.30	3.607	2.04	0.59	0.02
	3.572	2.06	0.58	0.03
	3.536	2.08	0.57	0.04
0.35	3.536	2.04	0.57	0.02
	3.501	2.06	0.56	0.03
	3.466	2.02	0.55	0.01

Table 3 shows the major strain and minor strain in straight groove test under biaxial stretching condition. These strain values are for different depth increments and along the rolling direction.

Table 3. Strain values for straight groove test along rolling direction under biaxial stretching condition

Biaxial stretching condition				
Step depth (mm)	Major diameter (mm)	Minor diameter (mm)	Major strain	Minor strain
0.15	2.781	2.726	0.33	0.31
	2.809	2.754	0.34	0.32
	2.866	2.699	0.36	0.3
0.20	2.754	2.726	0.32	0.31
	2.781	2.672	0.33	0.29
	2.809	2.646	0.34	0.28
0.25	2.781	2.699	0.33	0.3
	2.809	2.672	0.34	0.29
	2.726	2.725	0.31	0.31
0.30	2.754	2.646	0.32	0.28
	2.781	2.593	0.33	0.26
	2.726	2.672	0.31	0.29
0.35	2.672	2.593	0.29	0.26
	2.699	2.568	0.3	0.25
	2.726	2.542	0.31	0.24

From the Forming Limit Diagram (Figure 7) for SPIF of AA 6061, 1 mm thick sheet along the rolling direction, the relation between the major and minor strain is obtained as follows:

$$\epsilon_{\text{major}} + \epsilon_{\text{minor}} = 0.62 \quad \dots (3)$$

The limiting strains for Al 6061 under all strain conditions in conventional forming were found by Djavanroodi and Derogur [19]. In this work, the limiting strains achieved in conventional forming and in SPIF were compared. For AA 6061 alloy sheet with 1 mm thickness, the limiting strain in SPIF under plane strain condition is almost 3 times greater. The reason for this increase is the low rate of strain in each pass and elimination of effect of strain hardening during the process. Similarly, the limiting strain in SPIF under biaxial strain condition is almost 1.5 times greater.

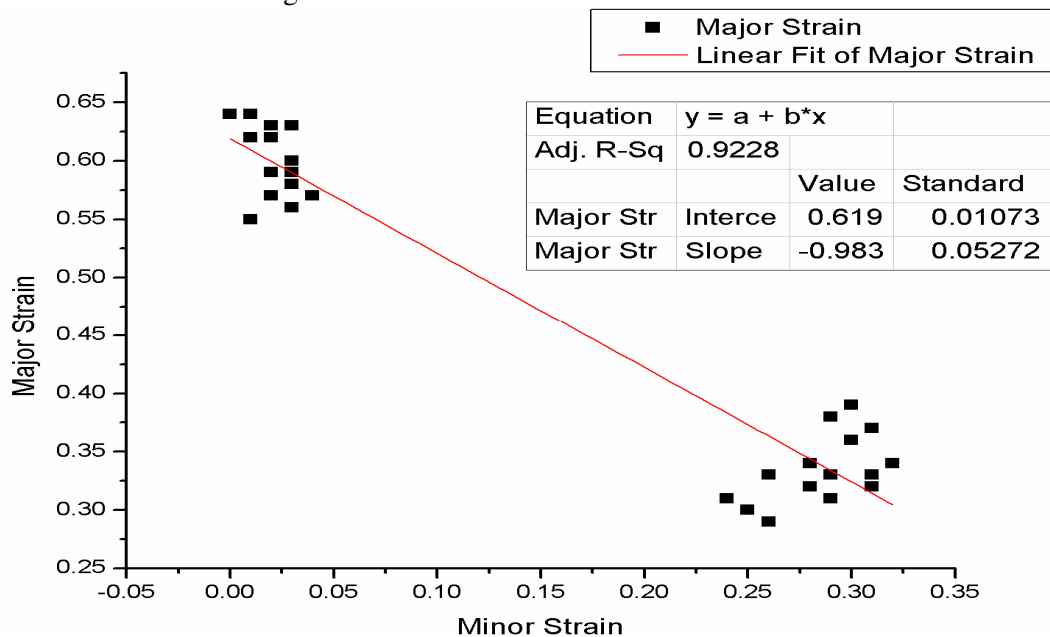


Figure 7. Forming limit diagram for SPIF of AA 6061, 1mm thick sheet (developed by straight groove test along rolling direction)

Comparing the sum of strain ($\epsilon_{\text{major}} + \epsilon_{\text{minor}}$) in plane strain condition and that in biaxial tension condition, the sum of the strain in plane strain condition shows a higher value. The reason for this is rapid rate of thinning due to the stretching in both axes. The forming limit curve for SPIF is shown in Figure 7. It is quite different from the curve for the conventional forming. It appears as a straight line with a negative slope of -0.983 in biaxial strain region. The value R^2 is a fraction between 0.0 and 1.0 that represents the variance of the errors among the data. When R^2 equals 1.0, all points lie exactly on a straight line with no scatter. With R^2 value of 0.9228, it is evidenced that all points lie on a straight line with very minimum variation. There is no negative strain (compressive strain) in any part of the groove. The reason is that the ball ended tool presses the sheet metal locally under its surface and the deformation is very small. Due to the nature of movement of the ball ended tool i.e., the tool first penetrates in the sheet metal and moved in one direction, the metal always flows away from the tool, that too in the direction of tool movement. Therefore the negative strain does not come into picture in any stage.

3.3 Straight groove test in Transverse Direction

Table 4 shows the major strain and minor strain in straight groove test under plane strain condition. These strain values are for different depth increments and along the transverse direction.

Table 4. Strain values for straight groove test along transverse direction under plane condition

Plain strain condition				
Step depth (mm)	Major diameter (mm)	Minor diameter (mm)	Major strain	Minor strain
0.15	3.680	2.02	0.61	0.01
	3.717	2.04	0.62	0.02
	3.755	2.02	0.63	0.01
0.20	3.607	2.04	0.59	0.02
	3.572	2.06	0.58	0.03
	3.644	2	0.6	0
0.25	3.572	2.04	0.58	0.02
	3.501	2.06	0.56	0.03
	3.572	2.02	0.58	0.01
0.30	3.466	2.020	0.55	0.01
	3.501	2.102	0.56	0.05
	3.432	2.081	0.54	0.04
0.35	3.466	2.02	0.55	0.01
	3.432	2.04	0.54	0.02
	3.466	2.10	0.55	0.05

Table 5 shows the major strain and minor strain in straight groove test under biaxial stretching condition. These strain values are for different depth increments and along the transverse direction.

From the forming limit diagram (Figure 8) for SPIF of AA 6061, 1 mm thick sheet along the transverse direction, the relation between the major and minor strain is obtained as follows:

$$\epsilon_{\text{major}} + \epsilon_{\text{minor}} = 0.58 \quad \dots (4)$$

The FLD shown in Figure 8 appears as a straight line with a negative slope of -1.080 in the positive region of the minor strain. Also the R^2 value of 0.9379 proves once again how all points lie on a straight line with very minimum variation. From these two curves (Figure 7 & 8), it is clear that the anisotropy property influences the incremental formability. However, in a real SPIF process the forming tool may moves along any direction varying from rolling direction to transverse. So the FLD for transverse direction is superimposed over the FLD for rolling direction to find the safe region as shown in Figure 9.

3.4 Depth of Groove Formed in Straight Groove Test

The depth of groove formed in straight groove test is also an indication of formability. This depth of groove values in straight groove test along rolling direction and transverse direction are tabulated in Table 6.

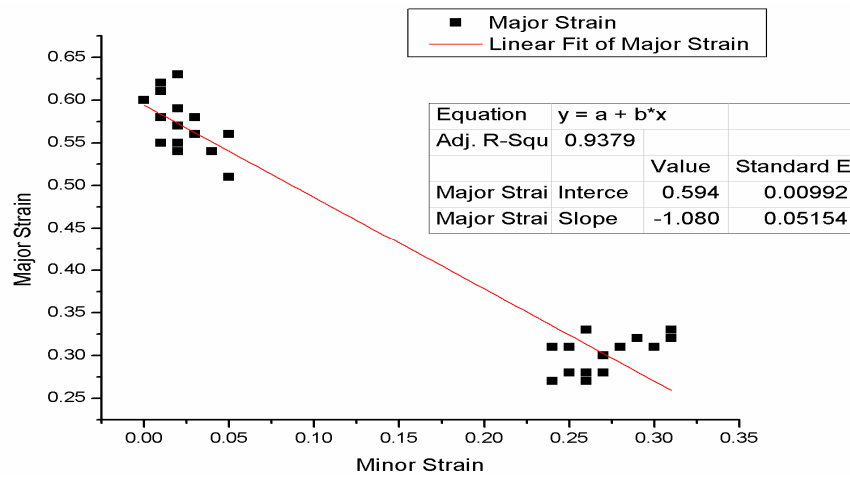


Figure 8. Forming limit diagram for SPIF of AA 6061, 1 mm thick sheet (developed by straight groove test along transverse direction)

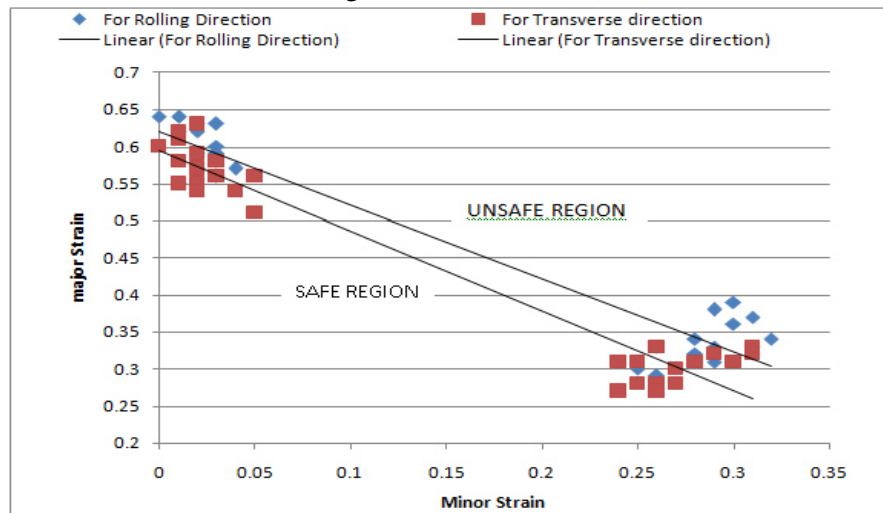


Figure 9. Combined FLD for rolling direction and transverse direction

Table 5. Strain for straight groove test along transverse direction under biaxial tension condition

Biaxial stretching condition				
Step depth (mm)	Major diameter (mm)	Minor diameter (mm)	Major strain	Minor strain
0.15	2.754	2.726	0.32	0.31
	2.726	2.699	0.31	0.3
	2.781	2.726	0.33	0.31
0.20	2.699	2.672	0.3	0.29
	2.726	2.646	0.31	0.28
	2.781	2.593	0.33	0.26
0.25	2.640	2.568	0.28	0.25
	2.619	2.593	0.27	0.26
	2.699	2.568	0.3	0.25
0.30	2.646	2.619	0.28	0.27
	2.699	2.619	0.3	0.27
	2.726	2.542	0.31	0.24
0.35	2.619	2.542	0.27	0.24
	2.619	2.593	0.27	0.26
	2.646	2.568	0.28	0.25

Table 6. Depth of the groove in straight groove test

Step depth (mm)	Depth of groove (mm)	
	In rolling direction	In transverse direction
0.15	9.15	8.7
0.20	9.0	8.6
0.25	8.75	8.25
0.30	8.40	7.8
0.35	8.05	7.35

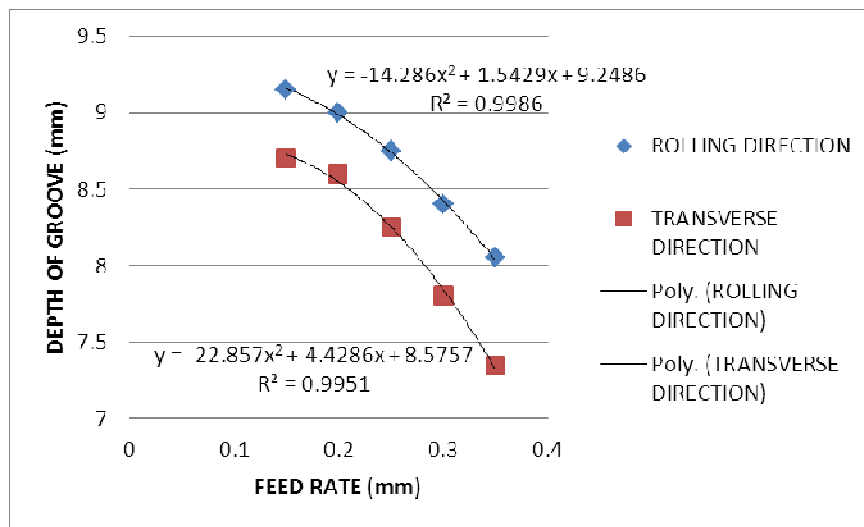


Figure 10. Effect of step depth on the formability in SPIF

From the plot between step depth and depth of groove (Figure 10), it is observed that higher the step depth, lower is the depth of forming. While the step depth increases, the severity of the forming increases. Therefore the depth of groove at fracture decreases. This is an indication for the reduction in formability. The effect of step depth on the depth of groove seems higher in transverse direction. The R^2 value of 0.99 obtained in both curves proves that the variation between the data is very minimum.

3.5 Cupping Test

The result of cupping test is given in Table 7. The FLD is drawn from the strain values. It is shown in Figure 11. Both FLDs developed from the incremental cupping test and incremental straight groove test gave higher limiting strain values than conventional FLD. From the FLD of cupping test, the relation between the major and minor strain is obtained as follows:

$$\epsilon_{\text{major}} + \epsilon_{\text{minor}} = 0.72 \quad \dots (5)$$

But the conditions simulated by the cupping test are much more realistic than the straight groove test. While comparing the forming limit strains of conventional and ISF, it is clear that the incremental forming limit strains are very well above the forming limit strains of conventional forming. From the incremental cupping test, it was also clear that the limiting wall angle of the cup formed is 53° .

Conclusion:

The annealed AA 6061 alloy sheet with 1 mm thickness was chosen for the formability analysis. The SPIF using ball ended tool was carried out using a CNC vertical milling machine. The straight groove and cupping tests were conducted and their FLDs in a peculiar pattern were plotted. Both FLDs show a well increased forming limit strains than the conventional forming limit strains. The FLDs plotted from the results of straight groove in rolling direction and transverse direction show that there is some effect of anisotropy in incremental sheet forming. The FLDs in this SPIF of AA 6061 is governed by the following equations:

1. $\epsilon_{\text{major}} + \epsilon_{\text{minor}} = 0.62$ (from straight groove test in rolling direction)
2. $\epsilon_{\text{major}} + \epsilon_{\text{minor}} = 0.58$ (from straight groove test in transverse direction)
3. $\epsilon_{\text{major}} + \epsilon_{\text{minor}} = 0.72$ (from cupping test)

It is also concluded that the formability decreases as the step depth increases during the SPIF. The research done on this paper may be further extended with spring back analysis and different materials. More process parameters can be included on the analysis to evaluate their influences on formability. Moreover, modelling of such process parameters may be carried for predicting the formability.

Table 7 Result of the cupping test

S. No.	Top diameter of truncated cone (mm)	Safe region		Failure region	
		Major strain	Minor strain	Major strain	Minor strain
1	112	0.59	0.01	0.38	0.35
		0.48	0.02	0.36	0.34
		0.36	0.04	0.37	0.34
		0.26	0.03	0.39	0.33
2	114	0.52	0.08	0.42	0.30
		0.43	0.07	0.43	0.28
		0.38	0.1	0.44	0.26
		0.18	0.11	0.46	0.27
3	116	0.45	0.15	0.48	0.24
		0.33	0.17	0.49	0.24
		0.28	0.12	0.46	0.25
		0.21	0.09	0.41	0.29
4	118	0.40	0.21	0.54	0.18
		0.32	0.18	0.56	0.14
		0.21	0.19	0.58	0.15
		0.17	0.14	0.58	0.15
5	120	0.39	0.20	0.60	0.12
		0.31	0.16	0.59	0.12
		0.18	0.15	0.62	0.08
		0.15	0.12	0.65	0.18
6	122	0.35	0.17	0.66	0.06
		0.25	0.13	0.72	0.04
		0.13	0.06	0.65	0.05
		0.11	0.09	0.64	0.09

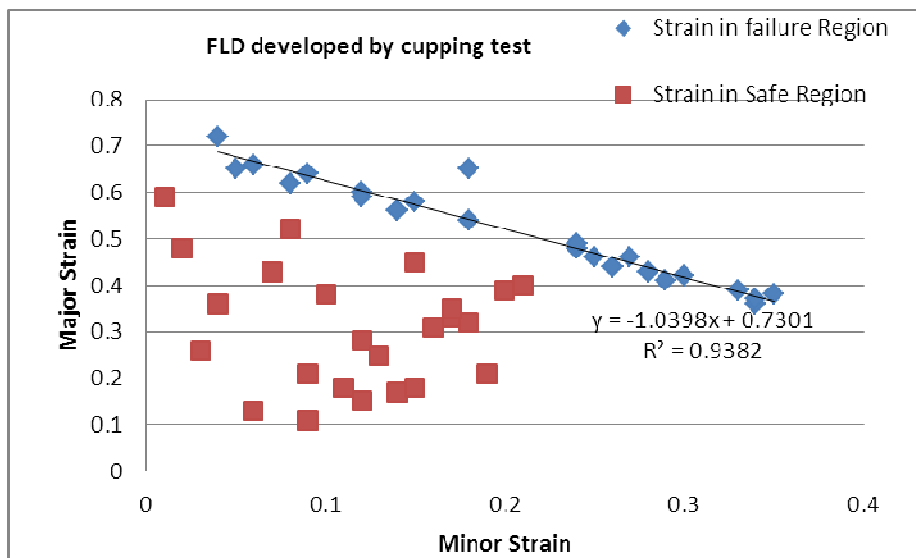


Figure 11. FLD of AA 6061 developed by incremental cupping Test

References

1. Narayanasamy R. and Sathiyarayanan C., Formability of HSLA and EDDQ steels of tube products of India, *Indian Journal of Engineering and Material Science*, 12 (2005) 141-150.
2. Kopac J and Kampus, Incremental sheet metal forming on CNC milling machine tool, *J. Mater. Process. Technol.* 162-163 (2005) 622-628.
3. Myoung-sup Shim and Jiong-jin park, The formability of aluminium sheet in incremental forming, *J. Mater. Process. Technol.*, 113 (2001) 654-658.
4. Matteo Strano, Technological Representation of Forming Limits for Negative Incremental Forming of Thin Aluminum Sheets, *J. Mater. Process. Technol.* 7, No 2 (2005) 122-129.
5. Hiroki Takano, Kimiyoshi Kitazawa, Teruyu Kigoto, Incremental forming of nonuniform sheet metal: Possibility of cold recycling process of sheet metal waste, *Int.j. mach tool manu.* 48 (2008) 477-482.
6. Toshiyuki Obikawa, Shunsuke Satou, Tomomi Hakutani, Dieless incremental micro-forming of miniature shell objects of aluminum foils, *Int.j. mach tool manu.*, 49 (2009) 906-915.
7. Yasunori Saotome and Takeshi Okamoto, An in-situ incremental microforming system for three-dimensional shell structures of foil materials, *J. Mater. Process. Technol.*, 113 (2001) 636-640.
8. Kim and Park, Effect of process parameters on formability in incremental forming of sheet metal, *J. Mater. Process. Technol.*, 130 (2002) 42-46.
9. Park J.J. and Kim Y.H., Fundamental studies on the incremental sheet metal forming technique, *J. Mater. Process. Technol.* 140 (2003) 447-453.
10. Kim T.T. and Yang D.Y., Improvement of formability for the incremental sheet metal forming process, *Int.j.mech.sci.* 42 (2000) 1271-1286.
11. Okoye C.N., Jiang C.N., Hu Z.D., Application of electromagnetic-assisted stamping (EMAS) technique in incremental sheet metal forming, *Int.j. mach tool manu.*, 46 (2006) 1248-1252.
12. Meier, Buff B., Laurischkat R., Smukala V., Increasing part accuracy in dieless robot based incremental sheet metal forming, *CIRP Annals – Manufacturing Technology*, 58 (2009) 233-238.
13. Minoru Yamashita, Manabu Gotoh, Shin-Ya Atsumi, Numerical simulation of incremental forming of sheet metal, *J. Mater. Process. Technol.* 199 (2008) 163-172.
14. Meier H., Magnus C., Smukala V., Impact of superimposed pressure on dieless incremental sheet metal forming with two moving tools, *CIRP Annals- manufacturing Technology* 60 (2011) 327-330.
15. Robert C., Delameziere A., Dal Santo P., Batoz J.L., Comparison between incremental deformation theory and flow rule to simulate sheet-metal forming processes, *J. Mater. Process. Technol.* 212 (2012) 1123-1131.
16. Murtha S.J., New 6XXX aluminum alloy for automotive body sheet applications, *SAE International Journal of Materials Manufacturing*, 104 (1995) 657-66.
17. Buha J., Lumley R.N., Crosky A.G., Microstructural development and mechanical properties of interrupted aged Al-Mg-Si-Cu alloy. *Metall. Mater. Trans. A.* 37A (2006) 3119-30.
18. Jeniski R.A. Jr., Effects of Cr addition on the microstructure and mechanical behavior of 6061-T6 continuously cast and rolled redraw rod, *Mater. Sci. Eng. A.* 237 (1997) 52-64.
19. Djavanroodi F., Derogar A., Experimental and numerical evaluation of forming limit diagram for Ti6Al4V titanium and Al6061-T6 aluminum alloys sheets, *Mater. Des.*, 31, No.10 (2010) 4866-4875.

(2015) ; <http://www.jmaterenvironsci.com>